第 33 卷第 12 期　　焊　接　学　报　　Vol. 33　No. 12
2012 年 12 月　　TRANSACTIONS OF THE CHINA WELDING INSTITUTION　　December　2012

搅拌摩擦焊接头形成过程分析

赵华夏，　董春林，　栾国红
（中国航空工业集团公司 北京航空制造工程研究所，北京　100024）

摘　要： 基于搅拌摩擦焊三维模型的切面分析方法，建立了焊接过程中接头切面的演变行为，将搅拌摩擦焊接头形成过程分为挤出阶段、迁移阶段、回填阶段和轴肩作用阶段四个阶段，对搅拌针作用下材料迁移过程进行了分析，指出挤出阶段将原始对接面及其表面氧化物迁移到后退侧，迁移阶段实现洋葱环层状组织的形成，并实现氧化物的碎化、弥散，回填阶段完成洋葱环形貌的最终成形. 结果表明，采用切面分析法建立的接头形成过程四阶段能够较好地解释搅拌摩擦焊接头形成机制以及“S 线”等缺陷的产生原因.

关键词： 搅拌摩擦焊；　切面分析；　接头成形；　缺陷
中图分类号： TG453　　**文献标识码：** A　　**文章编号：** 0253－360X(2012)12－0093－04

赵华夏

0　序　　言

搅拌摩擦焊(friction stir welding，FSW)凭借其具有的诸多优势，成为轻金属材料最先进的连接方法之一. FSW 焊接过程中，搅拌针周围被焊材料的产热、塑化及流动行为是形成接头的基础[1]. 因此国外学者针对 FSW 塑性金属流动行为开展大量研究工作，采用的研究方法包括示踪法[2]、急停法[3]、微观组织观察[4]或者多种方法相结合[5]. 国内也对塑性金属流动行为开展大量研究工作. 文献[6，7]构建了 FSW 塑性金属的层状流动模型. 文献[8]通过示踪试验研究得出“抽吸－挤压”理论. 文献[9]采用紫铜作为示踪材料研究了 FSW 焊接过程中塑性金属在水平面上的二维流动行为. 文献[10]采用铝箔示踪法研究了 FSW 洋葱环形成机制.

纵观国内外学者所开展的研究工作，不论采用何种试验方法，其研究视角基本都立足于焊接过程中塑性金属在搅拌针周围的流动轨迹. 而 FSW 焊接过程中塑性金属流动行为是不可见的，只能通过各种手段保留焊后接头内部的流动形貌，并通过切面金相照片体现出来，通过焊接终止后的二维图像去反推焊接过程中的三维运动行为必然存在极大的难度，并且分析结果与实际情况的吻合度也难以评判.

由于 FSW 接头理论上是由无数个二维切面叠加而成，而通过对接头切面的金相观察和分析来推断二维形貌的成形过程相对于推断搅拌针周围塑性金属的三维流动行为更为容易. 因此以下介绍的研究工作通过对单个切面的材料流动及成形过程分析来研究 FSW 接头成形机理.

1　FSW 模型建立

针对厚度为 6.35 mm 的 7050-T7451 铝合金 FSW 过程中实际使用的搅拌头及试件形貌进行建模，图 1 为实际焊接过程中搅拌针与被焊工件的相对位置关系，图 1 中隐藏了对接焊其中一侧工件，以便能够同时显示搅拌针及被焊工件形貌. 在被焊工件中选择任一切面 A(图 1)，并使切面 A 相对工件固定，观察任意时刻切面 A 处搅拌头与被焊工件的相互作用关系及其演变过程，观察方向如图 1 中虚线箭头所示.

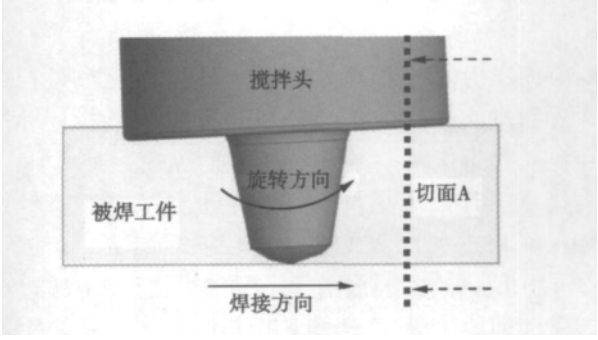

图 1　FSW 焊接过程模型
Fig. 1　Model of FSW process

从搅拌针根部接触到切面 A 开始，直至最终整

收稿日期：2012－06－18
基金项目：北京市科技计划资助项目(D111100002311002)

个搅拌针前缘完全越过切面 A，这个过程中 4 个不同阶段形貌如图 2 所示. 可以看到，随着搅拌头沿焊缝的直线运动，搅拌针根部首先进入切面 A，随后搅拌针作用区的长度及宽度都不断增大，当搅拌针端部进入到切面 A 后，搅拌针作用区长度基本不再发生明显变化，而宽度则缓慢增大，直至宽度最大值，即搅拌针直径. 由于焊接过程中搅拌针存在 2.5°的倾角，因此沿焊缝深度方向不同位置处搅拌针影响区宽度达到最大值的时刻并不相同，其先后次序为由下至上.

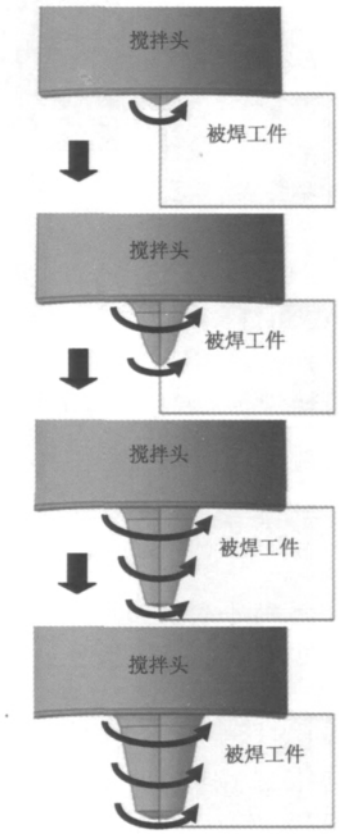

图 2 搅拌针进入切面 A 过程示意图

Fig. 2 Schematic of stir pin to enter section A

图 3 为搅拌针远离截面 A 的过程，远离过程可以看做进入过程的逆过程，在这个过程中，搅拌针作用区长度迅速减小，同时作用宽度也在不断减小.

基于对 FSW 模型的分析，将切面 A 中搅拌针作用区面积迅速增大的过程定义为挤出阶段，位于图 4 中 I 区，将搅拌针作用区面积迅速减小的过程定义为回填阶段，位于图 4 中 III 区，在上述两个阶段之间，搅拌针作用区变化不大，形成一个较为稳定的迁移过程，定义为迁移阶段，位于图 4 中 II 区，由于上述三个阶段均在搅拌针作用下完成，因此可以统称为搅拌针作用阶段. 从回填阶段结束到搅拌头

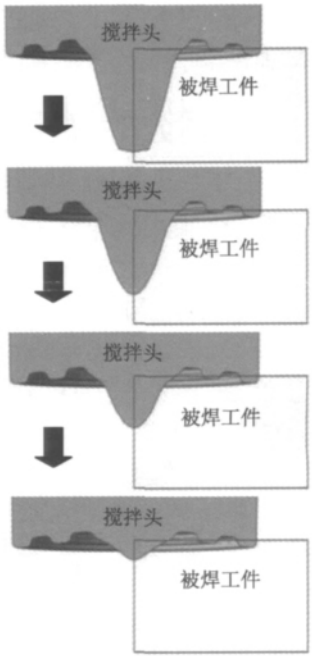

图 3 搅拌针退出切面 A 过程示意图

Fig. 3 Schematic of stir pin to exit section A

轴肩完全离开切面 A 这个过程定义为轴肩作用阶段.

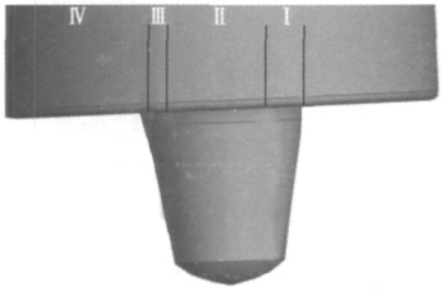

图 4 FSW 焊接过程四个阶段划分

Fig. 4 Stages of FSW process

2 FSW 焊接过程分析

在挤出阶段，焊缝靠近上表面的材料首先形成由前进侧(AS)向后退侧(RS)迁移行为，随着搅拌针作用区范围由搅拌针根部逐渐向端部扩展，焊缝区材料自上而下依次形成由前进侧向后退侧迁移行为，且上部的迁移宽度逐渐增大(图 5). 对接焊缝原始界面及其表面氧化物在该阶段被迁移至后退侧.

当搅拌针前缘完全越过截面 A 时，即进入迁移阶段，迁移阶段搅拌针作用区所占据的面积最大，同时迁移阶段与挤出阶段和回填阶段相比持续的时间也最长. 在该阶段，沿搅拌针外轮廓形成 FSW 接头

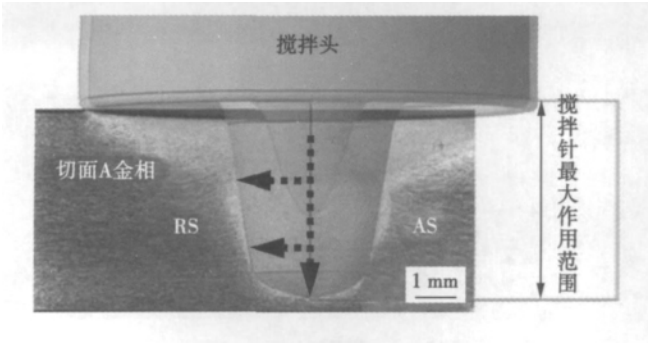

图 5　挤出阶段材料流动行为

Fig. 5　Material flow behavior of extrusion stage

热力影响区及焊核区的初步轮廓，同时该阶段是洋葱环层状组织的形成阶段，洋葱环芯以下部位在此阶段完全成形，与焊后切面 A 金相形貌相一致（图 6 中虚线框所示）. 随着洋葱环结构的形成，挤出阶段由原始界面迁移到后退侧的氧化物被碎化并沿洋葱环层状结构弥散分布于焊核中. 当搅拌针作用区底部回缩至洋葱环芯位置时，迁移阶段结束，随即进入回填阶段.

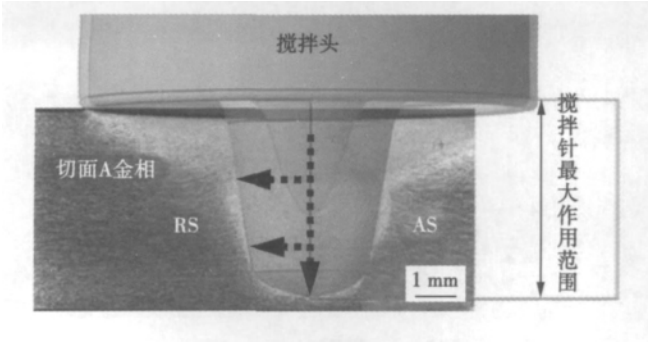

图 6　迁移阶段结束及回填阶段开始时刻切面 A 形貌

Fig. 6　Section A morphology between migration stage and back filling stage

图 7 为迁移阶段搅拌针作用区面积达到最大时，作用轮廓与金相形貌叠加. 图 7 中实线为焊核区边界，椭圆圈住的 a，b 区与搅拌针边缘的距离在该时刻达到最小，在该时刻之前和之后均远离搅拌针，因此可以认为该时刻是 a，b 区域焊缝成形的主要阶段，保留了迁移阶段搅拌针周围材料形貌. 图 7 中两条虚线为 a，b 焊核区边界向上的延伸，可以推断，在搅拌针作用区面积达到最大时刻，搅拌针两侧的塑性金属分布范围应当如虚线所界定的区域，但由于随后轴肩对上表面材料形成的迁移、挤压作用，使得迁移阶段在上部形成的焊核形貌被破坏，并且被轴肩作用区所取代.

回填阶段是焊核成形的关键阶段，其过程也相对复杂. 首先，回填阶段的起始点并非搅拌针作用区面积达到最大值时刻. 因为在搅拌针作用区面积达到最大值之后一段较短时间内，由于搅拌针作用区面积变化比（即搅拌针作用区面积单位时间缩小量与总面积的比值）较小，通过塑性金属的迁移行为尚且可以填充于搅拌针作用区缩小形成的新空隙，因此可以不断形成新的洋葱环，因此这个过程也归类于迁移阶段. 当搅拌针作用区尖端达到洋葱环芯位置（图 6）后，搅拌针作用区面积变化比迅速增大，迁移形成的塑性金属材料已经不足以填充新产生的空隙，为了填补空隙，迁移阶段在焊缝上部形成的塑性金属区及热力影响区材料开始向焊缝中心回填，此时不再产生新的洋葱环，而是将原有的层状组织收拢、闭合，构成洋葱环形貌的上半部，并形成最终完整的洋葱环形貌.

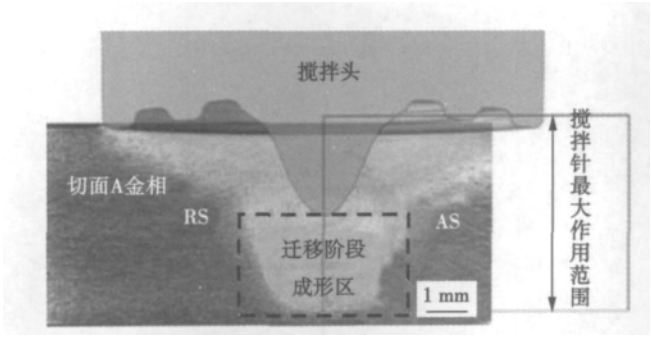

图 7　搅拌针作用区面积最大时切面 A 形貌

Fig. 7　Section A morphology at largest area of pin-affected zone

如图 8 所示，回填阶段形成的焊核区介于洋葱环芯及搅拌针作用区顶部之间一个较窄的区域内. 搅拌针作用区顶部及洋葱环结构的收拢形成于轴肩作用区塑性金属的挤压，而洋葱环结构两侧拐点位置低于搅拌针作用区顶部，又表明回填阶段焊核区形貌的形成过程受到了搅拌针后部间隙的回抽作用，而使焊核区上部材料产生了主动收拢回填的效果. 这种主动回填与轴肩作用区产生的被动挤压如果不能良好配合则容易在该位置形成疏松或孔洞缺陷.

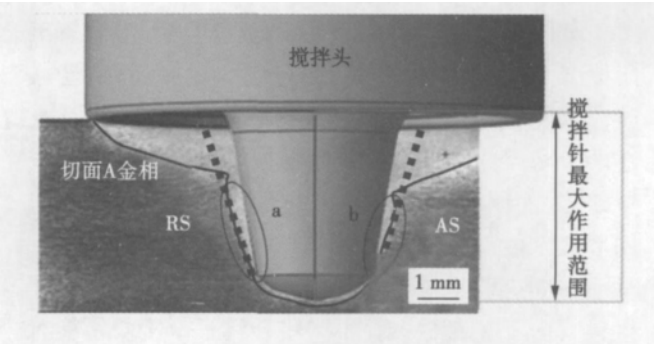

图 8　回填阶段成形区位置

Fig. 8　Forming position of back filling stage

如图9所示，由于工艺参数选择不当，导致挤出阶段未能对原始对接面形成有效的材料迁移，迁移阶段未能在焊核区下部形成良好的洋葱环形貌，上述两个阶段的共同影响从而形成了“S线”氧化物残留缺陷；而回填阶段在搅拌头下压量不足的共同作用下又未能产生主动回填与被动挤压的有效配合，从而在前进侧上部形成了孔洞缺陷. 由此可见，焊接过程中工艺参数选择不当将导致三个阶段不能有效完成各自的成形过程，而最终得到的缺陷焊缝往往是由各阶段产生的缺陷叠加而成.

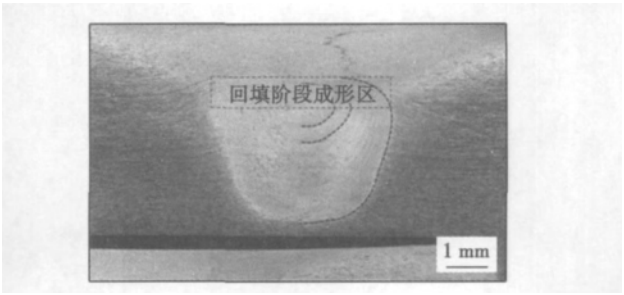

图9 缺陷焊缝金相形貌

Fig. 9 Metallograph of defective welded

3 结 论

(1) 基于切面分析法将搅拌针作用阶段划分为挤出阶段、迁移阶段和回填阶段.

(2) 挤出阶段搅拌针前缘自上而下将原始对接面上的材料由前进侧迁移至后退侧，对接焊缝原始界面及其表面氧化物在该阶段被迁移至后退侧.

(3) 迁移阶段沿搅拌针外缘轮廓形成焊核区边缘形貌以及洋葱环层状组织，后退侧氧化物在该阶段被部分碎化、弥散，分布于焊核区.

(4) 回填阶段形成洋葱环中心以上组织结构，并完成搅拌针作用区的最终形貌.

(5) 挤出阶段流动不充分易导致氧化层不能有效迁移，迁移阶段流动不充分易导致氧化层不能有效碎化弥散以及洋葱环不能有效形成，回填阶段流动不充分易导致隧道甚至沟槽缺陷.

参考文献：

[1] Threadgill P L, Leonard A J, Shercliff H R, *et al*. Friction stir welding of aluminium alloys [J]. International Materials Reviews, 2009, 54: 49 – 93.

[2] Lorrain O, Favier V, Zahrouni H, *et al*. Understanding the material flow path of friction stir welding process using unthreaded tools [J]. Journal of Material Processing Technology, 2010, 210: 603 – 609.

[3] Silva A A M, Arruti E, Janeiro G, *et al*. Material flow and mechanical behavior of dissimilar AA2024-T3 and AA7075-T6 aluminium alloys friction stir welds [J]. Materials and Design Mater, 2011, 32(4): 2021 – 2027.

[4] Cui Song, Chen Zhan. Effect of tool speeds and corresponding torque/energy on stir zone formation during friction stir welding/processing [J]. Material Science and Engineering, 2009, 4(1): 1 – 5.

[5] Schmidt H N B, Dickerson T L, Hattel J H. Material flow in butt friction stir welds in AA2024-T3 [J]. Acta Materialia, 2006, 54(4): 1199 – 1209.

[6] 王大勇，冯吉才，狄 欧，等. 铝合金搅拌摩擦焊接头焊核区等轴再结晶组织的形成机制 [J]. 焊接学报，2003，24(4)：33 – 35.
Wang Dayong, Feng Jicai, Di Ou, *et al*. Forming process analysis of equiaxed grain in weld nugget zone during friction-stir welding of aluminum alloy [J]. Transactions of the China Welding Institution, 2003, 24(4): 33 – 35.

[7] 王大勇，冯吉才. 搅拌摩擦焊接三维流动模型 [J]. 焊接学报，2004，25(4)：46 – 50.
Wang Dayong, Feng Jicai. 3 dimensional flow modeling of friction stir welding [J]. Transactions of the China Welding Institution, 2004, 25(4): 46 – 50.

[8] 柯黎明，潘际銮，邢 丽，等. 搅拌摩擦焊焊缝金属塑性流动的抽吸 – 挤压理论 [J]. 机械工程学报，2009，45(4)：89 – 94.
Ke Liming, Pan Jiluan, Xing Li, *et al*. Sucking-extruding theory for the material flow in friction stir welds [J]. Journal of Mechanical Engineering, 2009, 45(4): 89 – 94.

[9] 柯黎明，邢 丽，黄奉安. 搅拌摩擦焊接头形成过程的二维观察与分析 [J]. 焊接学报，2005，26(3)：1 – 4.
Ke Liming, Xing Li, Huang Feng'an. Two-dimensional flow of plasticized materials in friction stir welded joints [J]. Transactions of the China Welding Institution, 2005, 26(3): 1 – 4.

[10] 李宝华，唐众民，鄢江武，等. 搅拌头形状对搅拌摩擦焊接头中洋葱环形貌的影响 [J]. 热加工工艺，2010，39(19)：156 – 158.
Li Baohua, Tang Zhongmin, Yan Jiangwu, *et al*. Influence of tool shape on morphology of onion rings in welded joint during friction stir welding [J]. Hot Working Technology, 2010, 39(19): 156 – 158.

作者简介： 赵华夏，男，1980年出生，博士，工程师. 主要从事搅拌摩擦焊接机理及工艺研究. 发表论文9篇. Email: zhhq@sina.com

Abstract: Based on the section analysis of three-dimensional model of friction stir welding, the evolution of the joint section of the welding process was established. The forming process of friction stir welding was divided into extrusion stage, migration stage, backfilling stage and shoulder effect stage. The first three stages which were affected by stir pin were analyzed. The analysis of the material migration processes of the first three stages pointed out that the original surface and the residual oxides were migrated to the retreat side in the extrusion stage, the onion ring structure was formed, the oxides were fragmentated and dispersed in the migration stage and the onion ring structure was fully formed in the backfilling stage. The studies showed that if the above three stages could not effectively complete the forming processes, the superposition effect of a variety of defects forming mechanisms would lead to the formation of the final defects. The results show that the four stages of the forming process established by using the section analysis can be used to explain the forming mechanisms of FSW joints and the causes of the "S line" and other defects.

Key words: friction stir welding; section analysis; joint forming; defect

Effects of welding heat source parameters on residual stress and distortion in thin plate joint WANG Nengqing, TONG Yangang, DENG Dean (College of Materials Science and Engineering, Chongqing University, Chongqing 400045, China). pp 97 – 100

Abstract: The thermo-elastic-plastic finite element method (FEM) has been widely used to predict temperature field, residual stress distribution and deformation. However, how to choose the parameters of moving heat source model for given welding conditions heavily depends on a analyst's experience. It is necessary to clarify the influence of heat source parameters on residual stress and deformation. Therefore, an attempt was made to examine the influence of heat source parameters on residual stress and deformation in a thin plate joint using thermo-elastic-plastic FEM with Goldak heat source model in the current work. The simulation results show that the heat source parameters have no significant effect on residual stress, but have effect on welding deformation to some extent.

Key words: heat source; welding residual stress; welding deformation; numerical simulation

Effects of laser shock wave on salt spray corrosion of X70 pipeline steel welded lines WU Yongzhong, KONG Dejun, LONG Dan, FU Guizhong (College of Mechanical Engineering, Changzhou University, Changzhou 213016, China). pp 101 – 105

Abstract: The surface of X70 pipeline steel welded line was treated by laser shock wave, and the corrosion performances before and after laser shock processing were analyzed by salt spray corrosion test in artificial atmosphere. The surface morphologies, chemical elements and phase constituent were observed with SEM (scanning electron microscope), EDS (energy dispersive spectrometer) and XRD (X-ray diffraction), respectively, and the effects of laser shock processing on the corrosion mechanism were discussed. The results show that tensile residual stress exists in the surface of X70 pipeline steel welded lines in primitive state, which improves stress corrosion crack with the interaction of corrosive medium Cl^-. Spelling corrosion occurs with the interaction of boundary corrosion. The grain refinements are produced in the welded lines by laser shock processing, and the strengthened layer is formed on the surface, which improves corrosion resistance of the welded lines.

Key words: laser shock processing; X70 pipeline steel; welded line; salt spray corrosion

Characteristics of Ni-Cr-Co-W-Mo-Ta-B brazing filler LI Wen[1,2], JIN Tao[2] (1. College of Materials Science and Engineering, Shenyang Ligong University, Shenyang 110159, China; 2. Institute of Metal Research, Chinese Academy of Sciences, Shenyang 110016, China). pp 106 – 108

Abstract: Ni-Cr-Co-W-Mo-B alloy powder was prepared by gas atomization. The particle morphology and element distribution of the powder were investigated by SEM. The melting characteristics of the Ni-Cr-Co-W-Mo-Ta-B powder were evaluated by DSC. The Ni-Cr-Co-W-Mo-Ta-B flexible insert alloy cloth was obtained through a thermal rolling technology. The bonding strength at room temperature and stress rupture life at 1 010 ℃/248 MPa were measured. The results indicate that Ni-Cr-Co-W-Mo-Ta-B particles existas ball-shape and the element distributions are homogeneous in the particles. The liquidus temperature of the alloy is 1 127 ℃. The tensile strength at room temperature and stress rupture life at 1 010 ℃/248 MPa of the completed joints are almost identical to those of the superalloy substrate when the Ni-base superalloy was bonded by the transient liquid phase (TLP) bonding using Ni-Cr-Co-W-Mo-Ta-B powder as an insert alloy.

Key words: Ni-Cr-Co-W-Mo-Ta-B powder; Ni-base superalloy; TLP bonding; mechanical properties

Study of pulse combustion welding rod for vertical weld WU Yongsheng, WANG Jianjiang, XIN Wentong, LIU Haodong (The Institute of Advanced Materials, Ordnance Engineering College, Shijiazhuang 050003, China). pp 109 – 112

Abstract: A new type of manual SHS welding rod called the pulse combustion rod is introduced, which is used in the urgent repair of war. Firstly, the problems and insufficiency of the normal manual SHS welding rod (normal combustion rod for short) are analyzed in the vertical weld. The pulse combustion rod is designed with structure and constitution presented. Then vertical weld experiment is carried out, in which low carbon steel is used as the base metal. By analysis with SEM, XRD and EDS, the results show that weld seam is composed of Fe-riched phase and Cu-riched phase, with a few of α-Fe but a little of Fe-Ni, ε-Cu and Cu0.81Ni0.19 contained in Fe-riched phase, and with much ε-Cu but a little of Cu0.81Ni0.19, α-Fe and FeNi contained in Cu-riched phase. Dendritic Fe-riched phase distributes in the solid solution of Cu-riched phase. The weld seam alloy has a good bond with the base metal. The aim of double sides forming is obtained by single side welding. The mechanical properties test of weld joint presents that tensile strength is up to 367MPa and the hardness of weld alloying zone is 143.8 HV.

Key words: pulse combustion welding rod; vertical weld; microstructure and property